Laser wakefield acceleration in magnetized plasma

Pallavi Jha,[1] Akanksha Saroch,[1] Rohit Kumar Mishra,[1] and Ajay Kumar Upadhyay[2]
[1]*Department of Physics, University of Lucknow, Lucknow-226007, India*
[2]*Centre for Excellence in Basic Sciences, University of Mumbai, Mumbai-400098, India*
(Received 6 January 2012; published 1 August 2012)

A one-dimensional numerical model to study the evolution of longitudinal electrostatic wakefields, generated by propagation of a circularly polarized laser pulse in magnetized plasma has been presented. The direction of the external magnetic field is considered to be along as well as opposite to the axis of propagation of the laser pulse. Further, two-dimensional particle-in-cell code is used to obtain the generated wakefields. Separatrix curves are plotted to study the trapping and energy gain of an externally injected test electron, by the generated electrostatic wakefields, in the relativistic regime. Under appropriate conditions, an enhancement in the peak energy of an externally injected electron in magnetized plasma, as compared to the unmagnetized case, has been observed.

DOI: 10.1103/PhysRevSTAB.15.081301 PACS numbers: 52.38.Kd, 52.25.Xz

I. INTRODUCTION

The propagation of intense laser pulses in underdense plasma is relevant to a wide range of physical mechanisms. This includes relativistic optical guiding [1–3], harmonic generation [4,5], and excitation of large amplitude plasma waves for particle acceleration. The motion of plasma electrons is largely influenced by the ponderomotive force of a short laser pulse, which is responsible for generating large amplitude electrostatic wakefields. The acceleration gradient (≈ 100 MV/m) generated by conventional radio frequency linear accelerators (linacs) is limited, due to the breakdown of the waveguide structure. However, using plasma as a medium for particle acceleration has no electrical breakdown limit and is capable of sustaining high acceleration gradients (≈ 100 GV/m) [6]. Laser driven plasma based accelerators were originally proposed about three decades ago by Tajima and Dawson [7]. Since then many schemes of laser-plasma accelerators have been developed [8,9]. One such promising scheme is the laser wakefield accelerator (LWFA) in which an ultrashort, terawatt, high frequency laser pulse propagating through an underdense plasma excites a wake of plasma oscillations. A particle with an appropriate initial energy, injected into such a wave, can be trapped and accelerated by the electrostatic wakefield to attain energy up to several GeV [10–15].

Many interesting phenomena arise when an intense laser pulse propagates in magnetized plasma [16–18]. The effect of an external magnetic field on the generation of transverse wakefields, in the weakly relativistic limit, has been reported [19,20]. Cherenkov wakes are excited by short laser pulses propagating in magnetized plasma [21]. Recent simulation studies on the effect of constant [22] and pulsed [23] magnetic field, for the generation of wakefields, have been presented. Hosakai *et al.* [24] have experimentally demonstrated energy boosting in LWFA in the presence of external magnetic field. For high laser intensities ($a_0 \geq 3$), 2D numerical simulations have shown enhanced electron trapping by a static longitudinal magnetic field, in the bubble regime of laser wakefield acceleration [25]. Trigger and control of self-injection in LWFA in the presence of a static transverse magnetic field in the bubble regime has been studied by Vieira *et al.* [26].

In the present study, we have developed a novel, one-dimensional numerical model to analyze the excitation of longitudinal, electrostatic wakefields produced by the propagation of intense circularly polarized laser pulses in uniform plasma embedded in a magnetic field directed parallel as well as antiparallel to the direction of propagation of the laser pulse. The plasma is assumed to be cold so that, before the passage of the laser pulse, the plasma electrons are at rest and the external magnetic field does not affect them. Considering a broad laser beam, the excited longitudinal, electrostatic wakefield amplitude is analyzed in the one-dimensional limit. The amplitudes of the generated wakefields obtained via numerical study are then compared with the wakefields obtained with the help of 2D particle-in-cell (PIC) simulations. Further, trapping and energy gain (acceleration) of an externally injected test electron, by the generated wakefields under the influence of the external magnetic field, is studied.

The organization of the paper is as follows: In Sec. II, the fluid equations governing the generation of the wakefields have been formulated using quasistatic approximation. Section III includes the evolution and numerical analysis of the longitudinal, electrostatic wakefields generated via laser-magnetized plasma interaction with external magnetization along and opposite to the direction of propagation of the laser pulse and its comparison to the wakes generated

via 2D PIC simulations. In Sec. IV, the trapping and enhancement in the peak energy attained by the externally injected test electron in magnetized plasma is studied, and compared with the unmagnetized case. Section V presents the summary and discussion.

II. FORMULATION

Consider a cold, homogeneous, underdense plasma having ambient electron density n_o, embedded in a constant external magnetic field ($\vec{B}_0 = \sigma B_0 \hat{z}$, where $\sigma = \pm 1$). A circularly polarized laser pulse represented by the vector potential $\vec{A}_L = A(z,t)[\hat{x}\sin(k_0 z - \omega_0 t) - \hat{y}\cos(k_0 z - \omega_0 t)]$ (where k_0 and ω_0 are, respectively, the wave number and frequency of the laser pulse) is considered to be propagating through the plasma along the positive z direction. In the present study the electric and magnetic fields are taken to be of the form $\vec{E} = -\frac{1}{c}\frac{\partial \vec{A}}{\partial t} - \vec{\nabla}\Phi$ and $\vec{B} = \vec{\nabla} \times \vec{A}$, where $\vec{A}$ and Φ are, respectively, the vector potential of the laser pulse and the scalar potential of the generated field.

The set of basic nonlinear fluid equations describing the interaction of the laser pulse with cold, relativistic, uniformly magnetized plasma are

$$\frac{\partial(\gamma \vec{v})}{\partial t} + (\vec{v}\cdot\vec{\nabla})(\gamma\vec{v}) = -\frac{e}{m}\left(\vec{E} + \frac{\vec{v}}{c} \times (\vec{B} + \sigma \vec{B}_0)\right) \quad (1)$$

$$\frac{\partial n_e}{\partial t} + \vec{\nabla}\cdot(n_e \vec{v}) = 0 \quad (2)$$

$$\nabla^2 \Phi = k_p^2 (n_e - 1), \quad (3)$$

where $\gamma [= (1 - v^2/c^2)^{-1/2}]$ is the relativistic factor and $\vec{v}$ and n_e are the plasma electron velocity and density, respectively.

The plasma electron velocities may be considered to be a superposition of slow and fast components ($\vec{v} = \vec{v}_s + \vec{v}_f$), oscillating at the plasma [$\omega_p = (4\pi n_0 e^2/m)^{1/2}$] and laser ($\omega_0$) frequencies, respectively. With the help of the Lorentz force equation (1), the fast components of the transverse (v_{xf} and v_{yf}) and longitudinal (v_{zf}) velocities may be obtained from

$$\frac{\partial(\gamma v_{xf})}{\partial t} = \frac{e}{mc}\frac{\partial A_x}{\partial t} - \sigma \omega_c v_{yf} \quad (4a)$$

$$\frac{\partial(\gamma v_{yf})}{\partial t} = \frac{e}{mc}\frac{\partial A_y}{\partial t} + \sigma \omega_c v_{xf} \quad (4b)$$

and

$$\frac{\partial(\gamma v_{zf})}{\partial t} = 0, \quad (4c)$$

where $\omega_c (= eB_0/mc)$ is the cyclotron frequency. Simultaneous solutions of Eq. (4) give

$$u_{xf} = \frac{a\omega_0}{(\sigma\omega_c + \gamma\omega_0)}\sin(k_0 z - \omega_0 t) \quad (5a)$$

$$u_{yf} = -\frac{a\omega_0}{(\sigma\omega_c + \gamma\omega_0)}\cos(k_0 z - \omega_0 t) \quad (5b)$$

and

$$u_{zf} = 0, \quad (5c)$$

where $a (= eA/mc^2)$ and $u_{jf} (= v_{jf}/c, j = x, y, z)$ are the normalized amplitude and velocities, respectively. Equation (5) gives the relativistic quiver velocity of a plasma electron in the presence of a circularly polarized laser pulse and an axial magnetic field. In the absence of the magnetic field, Eqs. (5a) and (5b) reduce to the standard quiver velocity of the plasma electron in unmagnetized plasma. It may be noted that the direction (σ) of the magnetic field determines whether the presence of the field causes an increase or decrease in the quiver amplitude.

Equation (1) may also be used to obtain the governing equations for the evolution of the slow plasma electron velocities, as

$$\frac{\partial(\gamma v_{xs})}{\partial t} + v_{zs}\frac{\partial(\gamma v_{xs})}{\partial z} + v_{zf}\frac{\partial(\gamma v_{xf})}{\partial z} = -\sigma\omega_c v_{ys}, \quad (6a)$$

$$\frac{\partial(\gamma v_{ys})}{\partial t} + v_{zs}\frac{\partial(\gamma v_{ys})}{\partial z} + v_{zf}\frac{\partial(\gamma v_{yf})}{\partial z} = \sigma\omega_c v_{xs}, \quad (6b)$$

and

$$\frac{\partial(\gamma v_{zs})}{\partial t} + v_{zs}\frac{\partial(\gamma v_{zs})}{\partial z} = \frac{e}{m}\frac{\partial\Phi}{\partial z} - \frac{e}{mc}v_{xf}\frac{\partial A_x}{\partial z} - \frac{e}{mc}v_{yf}\frac{\partial A_y}{\partial z}. \quad (6c)$$

It is seen that the slow longitudinal velocity is driven by the laser field whereas the transverse velocities are independent of it. Since the fast longitudinal velocity (v_{zf}) is zero, the radiation-dependent term $[(v_{zf} \times \vec{B})_{x,y}]$ does not appear in Eqs. (6a) and (6b). Therefore the slow transverse velocities are expected to be zero.

III. NUMERICAL ANALYSIS OF LONGITUDINAL ELECTROSTATIC WAKEFIELD GENERATION

In order to study the evolution of longitudinal electrostatic wakefields, we first transform the slow components of the Lorentz force equation (6), continuity equation (2), and Poisson's equation (3), to a frame moving with the group velocity (v_g) of the laser pulse. These equations are hence written in terms of independent variables $\tau = t$ and $\xi = z - v_g t$. Since our present analysis is restricted to 1D, the transverse variations of the fluid quantities are not considered. Further, quasistatic approximation (QSA) is applied to the set of transformed fluid equations to study the slow evolution of wakefields. Under QSA, the field variations with respect to τ are neglected as the plasma electrons experience a static laser field [1]. The transformed normalized fluid equations (under QSA) are given by

$$\frac{\partial(u_{xs})}{\partial(k_p\xi)} = -\sigma\frac{\omega_c}{\omega_p}\frac{u_{ys}}{\gamma(u_{zs}-\beta_g)} - \frac{u_{xs}}{\gamma}\frac{\partial\gamma}{\partial(k_p\xi)} \tag{7a}$$

$$\frac{\partial(u_{ys})}{\partial(k_p\xi)} = \sigma\frac{\omega_c}{\omega_p}\frac{u_{xs}}{\gamma(u_{zs}-\beta_g)} - \frac{u_{ys}}{\gamma}\frac{\partial\gamma}{\partial(k_p\xi)} \tag{7b}$$

$$\frac{\partial(u_{zs})}{\partial(k_p\xi)} = \frac{1}{\gamma(u_{zs}-\beta_g)}\frac{\partial\phi}{\partial(k_p\xi)} - \frac{\omega_0}{2(\gamma\omega_0+\sigma\omega_c)(u_{zs}-\beta_g)} \times\frac{\partial a_0^2}{\partial(k_p\xi)} - \frac{u_{zs}}{\gamma}\frac{\partial\gamma}{\partial(k_p\xi)} \tag{7c}$$

$$\frac{\partial^2\phi}{\partial(k_p\xi)^2} = n-1 \tag{7d}$$

$$\frac{\partial n}{\partial(k_p\xi)} = -\frac{n}{(u_{zs}-\beta_g)}\frac{\partial u_{zs}}{\partial(k_p\xi)}, \tag{7e}$$

where $\phi(=e\Phi/mc^2)$ and $n(=n_e/n_o)$ are the normalized scalar potential of the generated wakefield and normalized plasma electron density, respectively. While deriving Eqs. (7a)–(7c), the fast velocities [Eq. (5)] have been used and the second harmonics of the laser frequency have been neglected. The normalized group velocity ($\beta_g = v_g/c$) of the laser pulse is derived from the dispersion relation, $c^2k_0^2 = \omega_0^2 - [\omega_p^2\omega_0/(\gamma\omega_0+\sigma\omega_c)]$ as

$$\beta_g = \frac{2[\omega_0^2 - \omega_0\omega_p^2/(\gamma\omega_0+\sigma\omega_c)]^{1/2}}{[2\omega_0 - \sigma\omega_c\omega_p^2/(\gamma\omega_0+\sigma\omega_c)^2]}. \tag{8}$$

Using the fourth-order Runge-Kutta algorithm, Eq. (7) can be simultaneously solved, with appropriate laser and plasma parameters, to give the wake potential and hence the wakefield $[E_{nz} = -\partial\phi/\partial(k_p\xi)]$. It may be noted that these equations are valid for arbitrary pulse profiles.

In order to analyze the generation of wakefields, we consider that the laser pulse has a Gaussian profile of the form $a = a_o\exp(-\xi^2/L^2)$, where a_0 is the laser strength parameter and L is the laser pulse length. Since the amplitude of the axial wakefield behind the trailing edge of the (Gaussian) laser pulse will tend to be maximum when the pulse length is approximately equal to $1/\pi\sqrt{2}$ times the plasma wavelength [27], therefore, for a plasma wavelength $\lambda_p = 32\ \mu$m $(n_0 = 1.09\times10^{18}/\text{cm}^3)$ we choose, the pulse length to be $L = 7.2\ \mu$m (pulse duration of 24 fs), for attaining maximum wakefield amplitude. The laser frequency is considered to be $\omega_0 = 2.355\times10^{15}$ Hz (corresponding to laser wavelength of 800 nm). Two regimes of laser intensity have been studied via the highly ($a_0 = 1.0$) and mildly ($a_0 = 0.3$) relativistic regimes.

As expected, the slow transverse velocities and hence transverse wakefields do not arise when the circularly polarized laser pulse interacts with axially magnetized plasma. Hence, only longitudinal electrostatic wakefields are generated and are affected by the external magnetic field. In Fig. 1 (Fig. 2), curves a, b, and c, respectively, show the variation of normalized wake potential with respect to $k_p\xi$, for $\sigma = -1$, 0, and $+1$ for $a_0 = 1.0$ (0.3)

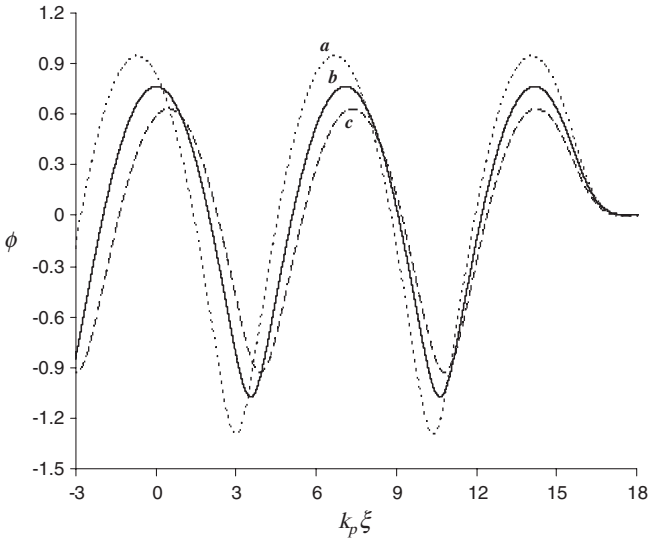

FIG. 1. Variation of normalized longitudinal electrostatic potential (ϕ) with $k_p\xi$ for $\sigma = -1$ (curve a), $\sigma = 0$ (curve b), and $\sigma = +1$ (curve c) for $a_0 = 1.0$, $\lambda_p = 32\ \mu$m, and $L = 7.2\ \mu$m.

and $\omega_c/\omega_p = 6$ ($B \approx 2000T$). Comparing Fig. 1 (Fig. 3) with Fig. 2 (Fig. 4) shows that the wake potentials (fields) generated in the relativistic ($a_0 = 1.0$) regime are enhanced tenfold with respect to the mildly relativistic ($a_0 = 0.3$) case. Sinusoidal wakefields are obtained in the mildly relativistic regime, whereas steepening of the wakefields is observed in the relativistic regime. It is seen that there is an enhancement of 24.5% (18.3%) in the wake potential obtained in the presence of a reversed magnetic field as compared to the unmagnetized case. However, a decrease

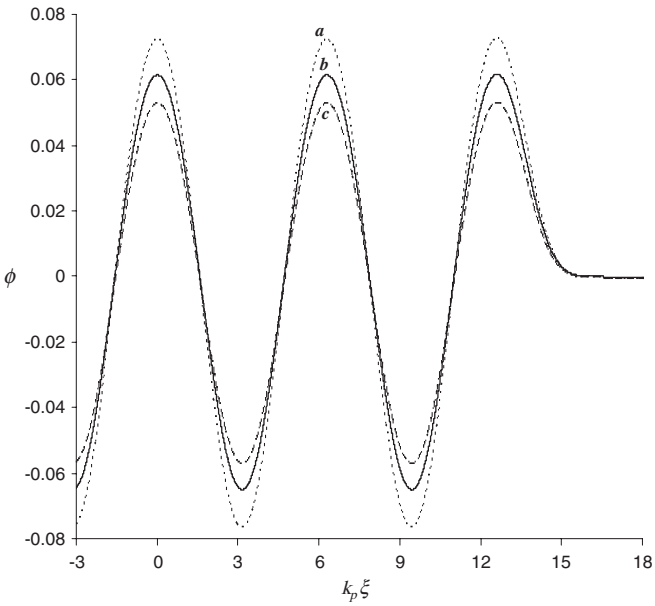

FIG. 2. Variation of normalized longitudinal electrostatic potential (ϕ) with $k_p\xi$ for $\sigma = -1$ (curve a), $\sigma = 0$ (curve b), and $\sigma = +1$ (curve c) for $a_0 = 0.3$, $\lambda_p = 32\ \mu$m, and $L = 7.2\ \mu$m.

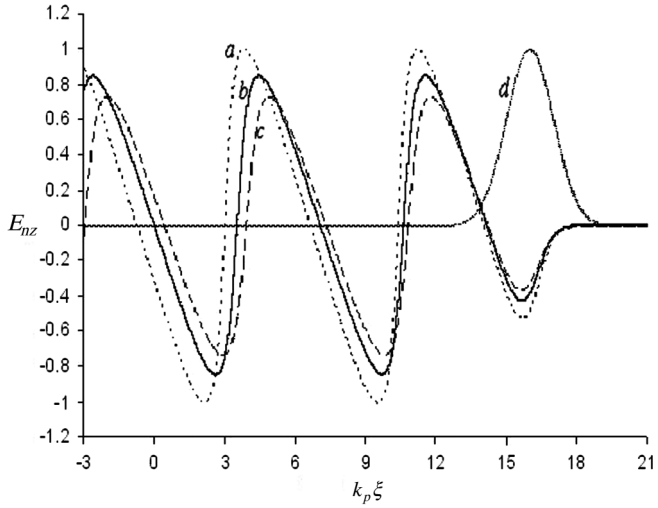

FIG. 3. Variation of normalized longitudinal electrostatic wakefield (E_{nz}) with $k_p\xi$ for $\sigma = -1$ (curve *a*), $\sigma = 0$ (curve *b*), and $\sigma = +1$ (curve *c*) for $a_0 = 1.0$, $\lambda_p = 32\ \mu$m, and $L = 7.2\ \mu$m. Curve *d* shows the evolution of the laser pulse.

of 16.7% (13.4%) is observed with a forward magnetic field. Similarly, Fig. 3 (Fig. 4) depicts the variation of normalized, longitudinal, electrostatic wakefield (E_{nz}) with $k_p\xi$, for the magnetized and the unmagnetized case for $a_0 = 1.0$ (0.3). An increase of 18.2% (17.6%) in the amplitude of the generated wakefield for $\sigma = -1$ and a decrease of 13.4% (13.1%) for $\sigma = +1$ in comparison to the unmagnetized case is seen. This shows that a reversed (forward) magnetic field increases (decreases) the amplitude of the generated axial wake potential and hence the wakefields.

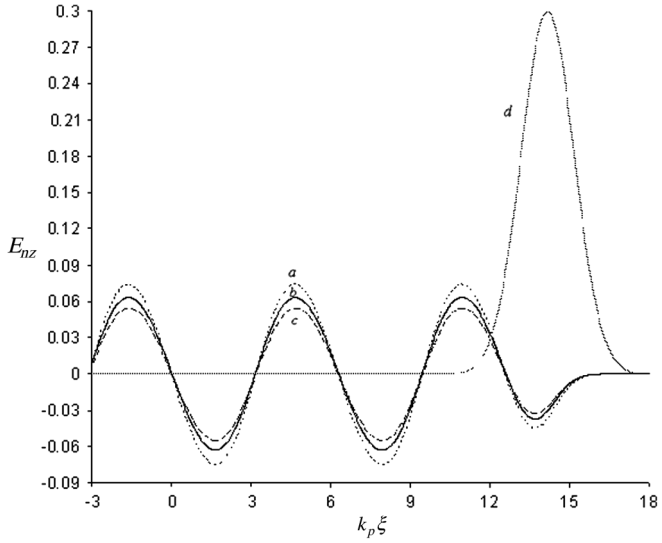

FIG. 4. Variation of normalized longitudinal electrostatic wakefield (E_{nz}) with $k_p\xi$ for $\sigma = -1$ (curve *a*), $\sigma = 0$ (curve *b*), and $\sigma = +1$ (curve *c*) for $a_0 = 0.3$, $\lambda_p = 32\ \mu$m, and $L = 7.2\ \mu$m. Curve *d* shows the evolution of the laser pulse.

Further, we have conducted simulations using two-dimensional PIC code, XOOPIC [28]. In the simulation process, a circularly polarized laser pulse having Gaussian temporal and radial profile was launched in a homogeneous magnetized plasma. The full width at half maximum (FWHM) pulse length $L_{\mathrm{FWHM}}(= \sqrt{2\ln 2}L)$ was considered to be 8.47 μm (FWHM pulse duration of 28.25 fs), corresponding to $L = 7.2\ \mu$m. The size of the simulation domain was 80 μm (this includes 20 μm vacuum distance) in the laser propagation direction (x) and 400 μm in the transverse direction (y). The domain is divided into 2048×512 meshes. The time step (satisfying the Courant condition) is taken to be 0.07 fs. We have assumed the transverse laser spot size (r_0) to be 80 μm in order to fulfill the broad beam ($k_p r_0 \gg 1$) condition so that our 1D numerical results are compatible with the simulation study. The ions form an immobile neutralizing background fluid. All other laser and plasma parameters are the same as those used for the numerical study.

In Fig. 5 (Fig. 6) curves *a*, *b*, and *c* are the simulation results showing the evolution of normalized longitudinal electrostatic wakefields with propagation distance (x) for reverse, zero, and forward magnetic fields, respectively, in the highly (mildly) relativistic regime. The simulation results show the same trend in the wakefield evolution curves as predicted via numerical study. However, the normalized peak values of the generated wakefield (E_{nx}) via simulation are seen to be suppressed as compared to the maximum wakefield amplitude obtained numerically. This may be attributed to 2D nonlinear effects. Another important 2D effect that may be noted is that the plasma wavelength (plasma density) increases (decreases) in the relativistic regime (Fig. 6) as compared to the mildly

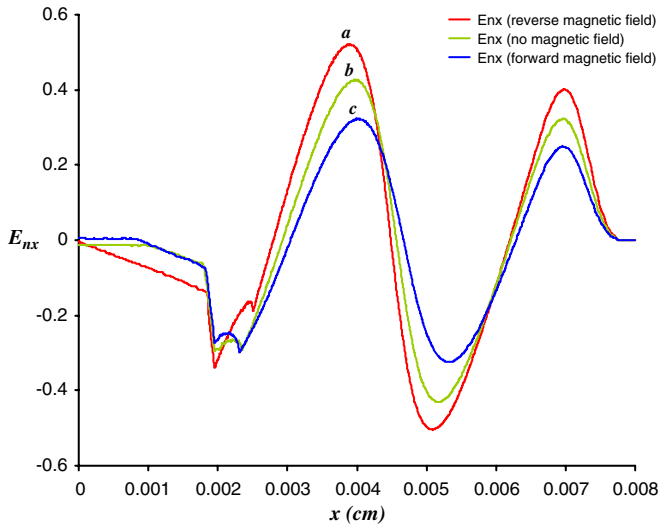

FIG. 5. Variation of normalized longitudinal electrostatic wakefield (E_{nx}) with x for $\sigma = -1$ (curve *a*), $\sigma = 0$ (curve *b*), and $\sigma = +1$ (curve *c*) for $a_0 = 1.0$ using 2D XOOPIC simulation code.

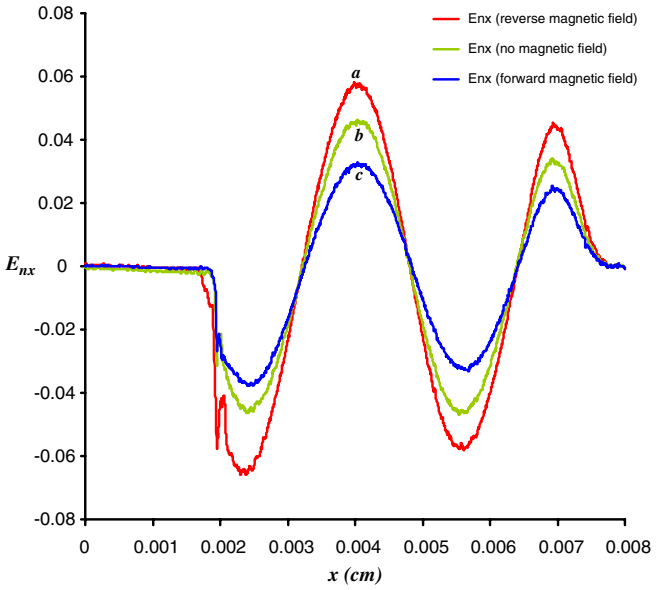

FIG. 6. Variation of normalized longitudinal electrostatic wakefield (E_{nx}) with x for $\sigma = -1$ (curve a), $\sigma = 0$ (curve b), and $\sigma = +1$ (curve c) for $a_0 = 0.3$ using 2D XOOPIC simulation code.

relativistic case (Fig. 5). This is due to the enhanced ponderomotive force that dominates in the relativistic regime.

IV. TRAPPING AND ACCELERATION OF A TEST ELECTRON

In order to study the acceleration mechanism, we consider a test electron to be injected behind the laser pulse. The exchange of energy between the generated axial wakefield and the test electron can be obtained with the help of Hamiltonian dynamics [29]. Assuming the system energy (Hamiltonian) to be conserved, we must have

$$H(\gamma_e, \Psi) = H(\gamma_i, \Psi) \text{ or } H(\gamma_e, \Psi_{\max}) = H(\gamma_p, \Psi_{\min}), \quad (9)$$

where the injection energy (γ_i) of the test electron, is considered to be equal to γ_p [$= (1 - v_p^2/c^2)^{-1/2}$, v_p is the phase velocity of the plasma wave] and γ_e represents the maximum energy attained by the test electron. $\Psi(= k_p\xi)$ is the phase of the test electron relative to that of the plasma wave. $\Psi_{\max}$ ($\Psi_{\min}$) in Eq. (9) represents the phase where the wake potential is maximum (minimum). An important characteristic of the phase space is the separatrix which separates the regions of trapped and untrapped electrons in the phase space. In order to plot the separatrices characterizing the just trapped test electron in the phase space, we inject the test electron at $\Psi_{\min}$ where the wake potential is minimum. Following Esarey and Pilloff [29], Hamilton's equation along with the energy conservation equation (9) leads to

$$\gamma_e(1 - \beta_e\beta_p) - \phi(\Psi) = \gamma_p(1 - \beta_p^2) - \phi_{\min}(\Psi_{\min}), \quad (10)$$

where β_e is the normalized final velocity associated with the accelerated test electron and $\beta_p = v_p/c$. The peak energy (γ_e) of the test electron can be obtained from Eq. (10) as

$$\gamma_e = \gamma_p(1 + \gamma_p\Delta\phi) \pm \gamma_p\beta_p[(1 + \gamma_p\Delta\phi)^2 - 1]^{1/2}, \quad (11)$$

where $\Delta\phi = \phi - \phi_{\min}$ and $\pm$ gives $\gamma_e(\max)$ and $\gamma_e(\min)$, respectively.

Assuming that the normalized phase velocity of the plasma wake (β_p) is equal to the normalized group velocity of the laser pulse (β_g), the separatrices of the test electron in the phase space bucket of the generated axial wakefield, for unmagnetized ($\sigma = 0$) and magnetized ($\sigma = \pm 1$, $\omega_c/\omega_p = 6$) plasma, are plotted by simultaneously solving Eqs. (7) and (11) using the fourth-order Runge-Kutta technique. Other laser and plasma parameters are the same as in Figs. 1–4. Figure 7 represents the separatrices of the test electron for unmagnetized and magnetized plasma, for $a_0 = 1.0$. In Fig. 7, the point of injection ($\phi_{\min}$, $\psi_{\min}$) of the test electron for tracing the separatrix for unmagnetized plasma (curve b) and magnetized plasma with $\sigma = -1$ (curve a) and $\sigma = +1$ (curve c) are, respectively (−1.075 60, 10.631), (−1.289 96, 10.376), and (−0.924 72, 10.801). The injection energy necessary for an electron to trace the separatrices a, b, and c in the phase space are, respectively, 22.5, 23.78, 25.69 MeV, while the maximum energies attained after acceleration are 4.5, 4.13, and 4.09 GeV, respectively. Hence, with a reduction (increase) of 5.68% (8.03%) in the injection energy, a gain (reduction) of 8.9% (0.96%) in

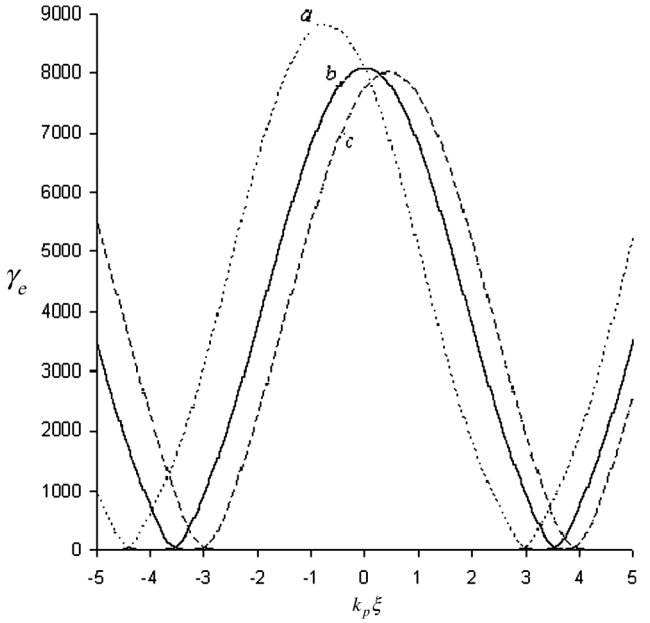

FIG. 7. Separatrix plots for the test electron with $\sigma = -1$ (curve a), $\sigma = 0$ (curve b), and $\sigma = +1$ (curve c), with injection energies, respectively, as 22.5, 23.78, and 25.69 MeV, for $a_0 = 1.0$.

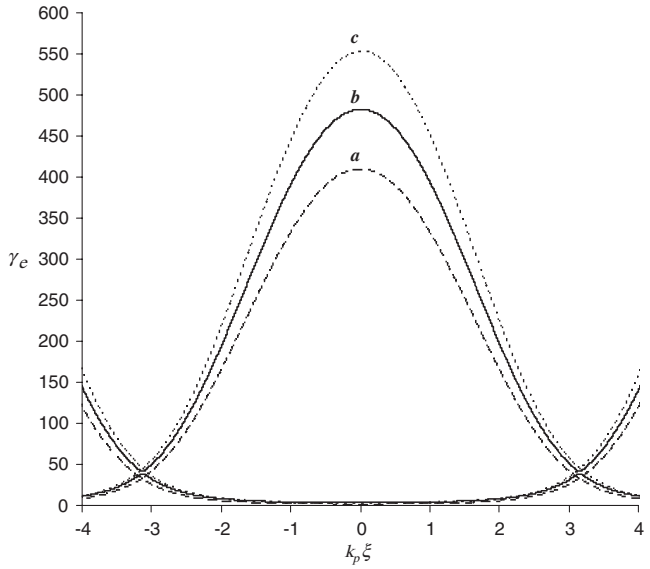

FIG. 8. Separatrix plots for the test electron with $\sigma = -1$ (curve *a*), $\sigma = 0$ (curve *b*), and $\sigma = +1$ (curve *c*), with injection energies, respectively, as 17.32, 20.43, and 23.47 MeV, for $a_0 = 0.3$.

the maximum energy of the accelerated test electron is seen for magnetized plasma with $\sigma = -1$ ($\sigma = +1$), in comparison to the unmagnetized case, while tracing the separatrix.

Similarly, Fig. 8 shows the separatrix plots for the mildly relativistic regime ($a_0 = 0.3$) for magnetized plasma with $\sigma = +1$ (curve *c*), $\sigma = -1$ (curve *a*), and unmagnetized plasma (curve *b*). For tracing the separatrices *a*, *b*, and *c*, the test electron is injected, respectively, at ($-0.076\,13$, 9.454), ($-0.065\,04$, 9.454), and ($-0.056\,76$, 9.454) with the injection energies 17.32, 20.43, and 23.47 MeV, respectively. It is observed that the maximum final energies of the accelerated test electron attained while tracing the separatrices *a*, *b*, and *c* are, respectively, 209.1, 245.8, and 282.5 MeV. Hence, a reduction (increase) of 17.5% (14.9%) is seen in the maximum final energy of the accelerated test electron for magnetized plasma with $\sigma = -1$ ($\sigma = +1$) as compared to the unmagnetized case. However, the injection energy for $\sigma = +1$ remains higher than that required for $\sigma = -1$.

It can be seen from Eq. (11), that the maximum final energy (γ_e) of the accelerated test electron depends upon the injection energy (γ_p) of the test electron as well as on the magnitude of the generated wake potentials. Therefore, for low magnitude of wake potential (as in the case of mildly relativistic regime), γ_e is predominantly determined by the injection energy (γ_p). Now, since the group velocity (and hence v_p and γ_p) of the laser pulse in magnetized plasma is greater for $\sigma = +1$ as compared to $\sigma = -1$ [Eq. (8)], higher energy of the accelerated test electron is obtained for forward as compared to the reversed magnetization case when $a_0 \ll 1$. On the contrary, for $a_0 \sim 1$, the final test electron energies are governed mainly by the high wake potential which is about tenfold greater than that in the mildly relativistic case. This leads to enhanced electron energy for reverse magnetic field as compared to the forward field.

In order to evaluate the effective gain in electron energy for each of the six cases under consideration, we define the gain $g = (\gamma_e - \gamma_p)/\gamma_p$. For $a_0 = 1.0$, the respective values of gain for $\sigma = -1$, 0, and $+1$ are 199.0, 172.6, and 158.2. However, for $a_0 = 0.3$, the gain is given by 11.06, 11.03, and 11.03 for $\sigma = -1$, 0, and $+1$, respectively. Thus, it is clear that effective enhancement of gain can be achieved for the highly relativistic regime with a reversed magnetic field. For the mildly relativistic regime, the presence of the magnetic field does not change the net gain in electron energy.

V. SUMMARY AND DISCUSSION

A one-dimensional numerical model for studying the generation of longitudinal electrostatic wakefields in the relativistic regime, by the propagation of a laser pulse in magnetized plasma, has been presented. The direction of external magnetization is considered to be along as well as opposite to the direction of propagation of the laser pulse. In order to highlight the effects of the applied magnetic field we have used large ($\sim$MG) values of the field. Conventionally, such intense magnetic fields are currently not realizable. However, under appropriate conditions, constant [30] and quasistatic [31–34] magnetic fields ($\sim$MG) are generated via laser-plasma interaction. Since these time-varying magnetic fields oscillate at the plasma frequency (which is much less than the laser frequency), the laser pulse interacting with plasma which is embedded in a quasistatic magnetic field will experience a nearly constant amplitude of the magnetic field. Such self-generated intense magnetic fields can be utilized in laser wakefield accelerators.

The nonlinear fluid equations, describing the interaction of the laser pulse with uniformly magnetized plasma, are transformed to the frame of the laser pulse. Further, the equations are reduced to a time independent form using the quasistatic approximation and solved numerically, to study the longitudinal, electrostatic wakefield generation in the highly as well as mildly relativistic regimes. It is seen that the slow transverse velocities and hence transverse wakefields do not arise. Longitudinal wakefields are however affected by the presence of the magnetic field. The variation of wake potential and electric field amplitude of the generated wakefield when the magnetic field is directed opposite to and along the direction of laser pulse propagation has been studied and compared to the unmagnetized case. It is observed that the wake potential and the amplitude of the longitudinal electrostatic wakefields for reversed (forward) magnetic field increases (decreases) as compared to the unmagnetized case for $a_0 = 1$ as well as

$a_0 = 0.3$. The numerically predicted results are then compared with 2D PIC simulations result which shows the same trend in the wakefield evolution curves as predicted via numerical study.

Further, numerical methods are used to evaluate the maximum energy attained by an externally injected test electron, due to the generated electrostatic wakefield, with reversed and forward applied magnetic fields, for the two laser intensity regimes. An increase in the final energy of the test electron is observed for wakefields generated via interaction of circularly polarized laser pulse with reversed (forward) magnetic field for $a_0 = 1$ ($a_0 = 0.3$).

It may be noted that for the highly relativistic regime ($a_0 \sim 1$) the maximum energy of the test electron increases (decreases) when the magnetic field is applied along the reverse (forward) direction, in comparison with the unmagnetized case. In addition, the injection energy ($= \gamma_p mc^2$) required for trapping and accelerating a test electron reduces (increases) when the reversed (forward) magnetic field is applied. Therefore for intense laser pulses, application of a reversed magnetic field leads to two advantages—an increment in the peak energy of an externally injected test electron along with a lower injection energy requirement. On the contrary, a magnetic field applied along the forward direction suppresses the wakefield and hence the peak energy of the test electron.

Further, for the mildly relativistic case ($a_0 = 0.3$), the wakefields are enhanced (suppressed) for the reversed (forward) magnetic field as before. However, it is interesting to note that in this case the peak energy of an injected test electron is higher (lower) for the forward (reversed) magnetic field case. This anomalous behavior may be attributed to the fact that the increase in the phase velocity of the wakefield ($\sim$ group velocity of the laser pulse) plays a more vital role in the mildly relativistic regime in comparison to a small increase in the wake potential, leading to a reduction in the maximum energy attained by the accelerated test electron with magnetic field applied along reverse direction.

It is important to note that in the mildly relativistic regime, the external magnetic field does not cause any enhancement in the effective energy gain by the test electron. However, for the highly relativistic regime, a significant enhancement in effective gain in energy by the test electron is obtained when a reversed magnetic field is applied. This study will be significant for the analysis of trapping and acceleration of a test electron in magnetized plasma.

ACKNOWLEDGMENTS

This work has been done with the financial support of Science and Engineering Research Council, Department of Science and Technology, Government of India. The authors are grateful to the organization for funding the research project (Project No. SR/S2/HEP-22/2009).

[1] E. Esarey, P. Sprangle, J. Krall, and A. Ting, IEEE J. Quantum Electron. **33**, 1879 (1997).
[2] G. Durfee III and H. M. Milchberg, Phys. Rev. Lett. **71**, 2409 (1993).
[3] H. M. Milchberg, T. R. Clark, C. G. Durfee III, T. M. Antonsen, and P. Mora, Phys. Plasmas **3**, 2149 (1996).
[4] H. A. Salih, R. P. Sharma, and M. Rafat, Phys. Plasmas **11**, 3186 (2004).
[5] P. Jha, R. K. Mishra, G. Raj, and A. K. Upadhyay, Phys. Plasmas **14**, 053107 (2007).
[6] E. Esarey, C. B. Schroeder, and W. P. Leemans, Rev. Mod. Phys. **81**, 1229 (2009).
[7] T. Tajima and J. M. Dawson, Phys. Rev. Lett. **43**, 267 (1979).
[8] E. Esarey, P. Sprangle, J. Krall, and A. Ting, IEEE Trans. Plasma Sci. **24**, 252 (1996).
[9] R. Bingham, J. T. Mendonca, and P. K. Shukla, Plasma Phys. Controlled Fusion **46**, R1 (2004).
[10] J. Faure, C. Rechatin, A. Norlin, A. Lifschitz, Y. Glinec, and V. Malka, Nature **444**, 737 (2006).
[11] T. Esirkepov, S. V. Bulanov, M. Yamagiwa, and T. Tajima, Phys. Rev. Lett. **96**, 014803 (2006).
[12] C. E. Clayton, K. A. Marsh, A. Dyson, M. Everett, A. Lal, W. P. Leemans, R. Williams, and C. Joshi, Phys. Rev. Lett. **70**, 37 (1993).
[13] W. P. Leemans, B. Nagler, A. J. Gonasalves, C. Toth, K. Nakamura, C. G. R. Geddes, E. Esarey, C. B. Schroeder, and S. M. Hooker, Nature Phys. **2**, 696 (2006).
[14] C. E. Clayton, J. E. Ralph, F. Albert, R. A. Fonseca, S. H. Glenzer, C. Joshi, W. Lu, K. A. Marsh, S. F. Martins, W. B. Mori, A. Pak, F. S. Tsung, B. B. Pollock, J. S. Ross, L. O. Silva, and D. H. Froula, Phys. Rev. Lett. **105**, 105003 (2010).
[15] S. P. D. Mangles, C. D. Murphy, Z. Najmudin, A. G. R. Thomas, J. L. Collier, A. E. Dangor, E. J. Divall, P. S. Foster, J. G. Gallacher, C. J. Hooker, D. A. Jaroszynski, A. J. Langley, W. B. Mori, P. A. Norreys, F. S. Tsung, R. Viskup, B. R. Walton, and K. Krushelnick, Nature (London) **431**, 535 (2004).
[16] P. Jha, R. K. Mishra, A. K. Upadhyay, and G. Raj, Phys. Plasmas **14**, 114504 (2007).
[17] N. Wadhwani, P. Kumar, and P. Jha, Phys. Plasmas **9**, 263 (2002).
[18] P. Jha, A. Saroch, and R. K. Mishra, Europhys. Lett. **94**, 15001 (2011).
[19] G. Brodin and J. Lundberg, Phys. Rev. E **57**, 7041 (1998).
[20] A. Holkundkar, G. Brodin, and M. Marklund, Phys. Rev. E **84**, 036409 (2011).
[21] J. Yoshii, C. H. Lai, T. Katsouleas, C. Joshi, and W. B. Mori, Phys. Rev. Lett. **79**, 4194 (1997).
[22] R. S. Bonabi and M. E. Abari, Phys. Plasmas **17**, 032101 (2010).
[23] D. N. Gupta, H. Suk, and M. S. Hur, Appl. Phys. Lett. **91**, 211101 (2007).
[24] T. Hosokai, A. Zhidkov, A. Yamazaki, Y. Mizuta, M. Uesaka, and R. Kodama, Appl. Phys. Lett. **96**, 121501 (2010).
[25] M. S. Hur, D. N. Gupta, and H. Suk, Phys. Lett. A **372**, 2684 (2008).

[26] J. Vieira, S. F. Martins, V. B. Pathak, R. A. Fonseca, W. B. Mori, and L. O. Silva, Phys. Rev. Lett. **106**, 225001 (2011).
[27] L. M. Gorbunov and V. I. Kirsanov, JETP **66**, 290 (1987) [http://www.jetp.ac.ru/cgi-bin/e/index/e/66/2/p290?a=list].
[28] J. P. Verboncoeur, A. B. Langdon, and N. T. Gladd, Comput. Phys. Commun. **87** 199 (1995).
[29] E. Esarey and M. Pilloff, Phys. Plasmas **2**, 1432 (1995).
[30] Z. M. Sheng and J. Meyer-ter-Vehn, Phys. Rev. E **54**, 1833 (1996).
[31] V. I. Berzhiani, S. M. Mahajan, and N. L. Shatashvili, Phys. Rev. E **55**, 995 (1997).
[32] L. M. Gorbunov, P. Mora, and T. M. Antonsen, Jr, Phys. Plasmas **4**, 4358 (1997).
[33] B. Qiao, X. T. He, and S. Zhu, Phys. Plasmas **13**, 053106 (2006).
[34] A. K. Upadhyay and P. Jha, Phys. Plasmas **15**, 093101 (2008).